Effects of quantum fluctuations on the photoinduced midgap absorption in an *MX* chain complex $[Pt(en)_2][Pt(en)_2Cl_2](BF_4)_4$ where en = ethylenediamine

Noritaka Kuroda and Masato Nishida*
Institute for Materials Research, Tohoku University, Katahira 2-1-1, Aoba-ku, Sendai 980-77, Japan

Masahiro Yamashita
Graduate School for Human Informatics, Nagoya University, Chikusa-ku, Nagoya 464-01, Japan
(Received 14 June 1995)

Long-lived midgap states are found to be induced efficiently in a substance of the mixed-valence *MX* chain complex $[Pt(en)_2][Pt(en)_2Cl_2](BF_4)_4$, where en = ethylenediamine, by irradiation with the 488-nm line of an Ar laser polarized perpendicular to the Pt-Cl chain bonds. If the temperature is changed between 10 and 250 K in the dark after laser irradiation, the near-infrared absorption bands due to the photoinduced states show pronounced changes in the spectral position, line shape, and intensity. The behaviors of the mean energy and the second and third moments of the *A* band at low temperatures can be interpreted well in terms of the quantum fluctuation with an eigenfrequency of the order of 0.01 eV. Above about 100 K, the mean energy and the second and third moments show anomalous temperature dependencies, suggesting that the midgap states walk randomly in shallow and periodic potential wells of the chainlike bonds.

I. INTRODUCTION

The title substance is an *MX* chain complex of platinum and has an orthorhombic crystal structure[1] isomorphous with the orthorhombic phase[2] of $[Pt(en)_2][Pt(en)_2Cl_2]$ $(ClO_4)_4$ where (en) is ethylenediamine, in which the physical properties have been studied extensively. This substance is obtained by replacing the counter ions ClO_4 of $[Pt(en)_2][Pt(en)_2Cl_2](ClO_4)_4$ by BF_4. The replacement of the counter ions causes only a small change in the lattice constants. In particular, the ratio of the Pt^{IV}-Cl^- to Pt^{II}-Cl^- distances of the chainlike valence-alternating bonds

$$\cdots\text{-}Cl^-\text{-}Pt^{II}\text{-}Cl^-\text{-}Pt^{IV}\text{-}Cl^-\text{-}\cdots$$

is 0.759 in the BF_4 salt, being very close to 0.750 in the ClO_4 salt. Correspondingly, the interband reflection spectra, which is due to the $Pt^{II} \rightarrow Pt^{IV}$ charge-transfer transition, of the two substances strongly resemble one another:[1] The reflection spectrum peaks around 2.8 eV in both substances, indicating that the fundamental energy gap is about 3 eV. This fact means that the electronic properties in these substances are similar to one another.

The unrenormalized energy gap could be higher than 3 eV, since the two substances have the strongest electron-lattice coupling of many *MX* chain complexes.[3,4] One may regard the chainlike bonds as a doubly degenerate charge-density-wave (CDW) state resulting from the electron-lattice coupling. According to experiments on magnetic resonance in the ClO_4 salt,[5-8] mobile kink solitons with spin of $S = \frac{1}{2}$ can be created by optical irradiation in the CDW state. The unpaired electron is confined in the photoinduced domain wall which joins mutually antiphased chains of the valence-alternating bonds: This paramagnetic domain wall has a valence structure of $Pt^{2.5}$-Cl^--$Pt^{2.5}$. One may infer from a simple topological consideration that the solitons are created through the electron-transferring relaxation process of the photoexcited electron-hole pairs or the charge-transfer excitons.[9-11] The spins and thus the domain walls appear to be fluctuating around their optimum sites even at liquid-helium temperatures.[6] At elevated temperatures they move through the CDW chain bonds in the manner of the thermally activated random walk.[5,8] As far as undoped crystals are concerned, only a very small amount of polarons, which should also have a spin of $S = \frac{1}{2}$, may coexist with solitons.[7]

In the ClO_4 salt, in concurrence with the appearance of the electron paramagnetic resonance (EPR) signal due to the spin solitons mentioned above, three optical-absorption bands *A*, *B*, and *B'* are induced in the near-infrared and visible regions below the subgap tail[12] of the intrinsic charge-transfer band; they appear around 1.6, 2.0, and 2.1 eV, respectively.[11,13,14] It has been confirmed recently that a very similar intragap absorption is induced by laser irradiation in the BF_4 salt, as well.[15] The shift of the *A* band relative to the charge-transfer band under hydrostatic pressure proves that the *A* band is literally a midgap band in both substances,[15,16] supporting the notion that the *A* band arises from spin solitons. In contrast to the cases of solitons and polarons in other *MX* chain complexes[10,17] and those in other quasi-one-dimensional materials such as *trans*-polyacetylene, the decay time of the photoinduced absorption in the ClO_4 salt is quite long, being 1–10 s even at room temperature, and infinitely long below 200 K. This feature is more distinctive in the BF_4 salt; the decay time of the *A* band reaches 1 min even at room temperature.[15]

Another remarkable aspect of the intragap bands is

that their half-widths are appreciably greater than the values expected in the usual adiabatic approximation.[18–20] Moreover, the line shape of the A band is asymmetric. These aspects are characteristic of localized states of a system with a strong electron-lattice coupling. Indeed, the temperature dependence of the peak energy and the line shape of the main band, A, in the ClO_4 salt exhibits a behavior reflecting that the photoinduced states undergo a quantum fluctuation around their optimum sites at low temperatures, and a thermally activated random walk at high temperatures,[21,22] in agreement with the findings by EPR.

In the present paper we study the photoinduced absorption in the BF_4 salt to obtain more information on the nature of the midgap states in MX chain systems with strong electron-lattice coupling. We focus our attention on the temperature dependence of the intensity, the mean energy, and the second and third moments of the photoinduced bands. In Sec. II the experimental procedures are described. The results are presented in Sec. III. Properties of the quantum fluctuations and random walk are discussed quantitatively in Sec. IV on the basis of the configuration-coordinate model. Section V summarizes the results.

II. EXPERIMENTAL PROCEDURES

Single crystals are grown by the evaporation method from the aqueous solution of chemically synthesized material.[23] The material of 0.6 g is dissolved in distilled water of 10 ml. The solution is evaporated at a rate of about 1 ml/day. When the solution is saturated, the evaporation rate is lowered down to about 0.5 ml/day to grow single crystals. All the processes are conducted at room temperature (22–24 °C). Crystals with a thickness of 50–100 μm are used for the present experiment.

The absorption spectrum is measured using an optical multichannel system. A tungsten-halogen lamp is used as the light source. Light of wavelengths longer than 520 nm is obtained with a glass filter, and is polarized parallel to the Pt-Cl chain axis b of the crystal by a Glan-Thompson prism. The light which is transmitted by the sample is dispersed with a polychromator (Ritu Applied Optic MC-30ND). The dispersed light is detected by a charge-coupled-device (CCD) camera (Photometrics PM512). The shutter of the CCD camera is synchronized with the shutter of the light source. The intensity of the light source and the exposure time are set as low as possible in order to avoid the photoexcitation effect due to the light source. The typical exposure time chosen to take an absorption spectrum is 0.2 s.

The temperature of the sample is controlled with a continuous flow cryostat (Oxford Instruments CF1204) and a temperature controller (Oxford Instruments ITC4). The 488-nm line of a cw Ar-ion laser is used to irradiate the sample. The laser beam is polarized perpendicular to the b axis to produce the midgap states homogeneously throughout the crystal.[21] The power of the laser beam is regulated to be 0.05–0.5 W/cm^2.

III. RESULTS

Prior to the laser irradiation the absorption spectrum of the pristine sample is measured at various temperatures between 10 and 300 K. Figure 1 shows examples of the results. The thickness of the sample is 70 μm. There appears a weak intragap band below the subgap tail of the $Pt^{II} \rightarrow Pt^{IV}$ charge-transfer band denoted as CT, showing that a certain amount of the intragap states are inherently contained in the crystal. This band is located around 1.6 eV, corresponding well to the A band in the ClO_4 salt due mainly to the spin solitons. However, features corresponding to the B and B' bands, which are assignable to charged solitons,[14] are absent.

If the sample is irradiated with the laser beam, the A band is strengthened efficiently depending on the intensity of the laser beam and temperature. The photoinduced component of the A band decays if the irradiation is discontinued. Its time evolution is nonexponential, as has been reported elsewhere.[15] The $1/e$ decay time is typically 1 min at room temperature, but increases by orders of magnitude as temperature decreases: For the case of the sample shown in Fig. 1 the decay time becomes about 20 h at 250 K, and about 60 h at 240 K. Hence, after irradiating the sample at 250 K for 20 s with a laser beam of about 0.1 W/cm^2, we measure the absorption spectrum in the dark at various temperatures below 250 K. Figure 2 shows the spectra taken at the same temperatures as shown in Fig. 1. In addition to the A band, a broad absorption corresponding to the B' band may be identified around 2.0 eV. Compared to the spectrum of the pristine sample at low temperatures, it would appear that the B' band is newly induced by the laser irradiation.

To obtain the net component of the photoinduced ab-

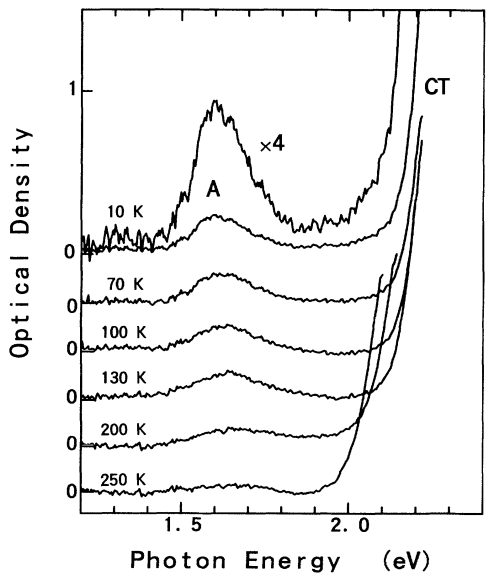

FIG. 1. Absorption spectra measured for polarization parallel to the chain axis b at various temperatures prior to the laser irradiation.

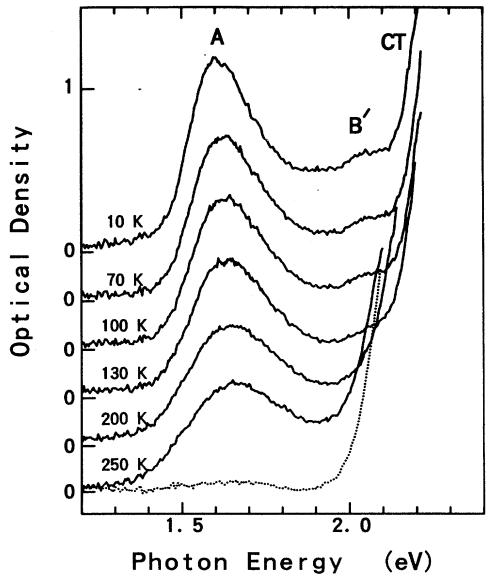

FIG. 2. Absorption spectra measured for polarization parallel to the chain axis b at various temperatures after the sample is irradiated at 250 K. The dotted curve is the spectrum taken at 250 K before irradiation.

sorption, the preirradiation spectrum is subtracted from the postirradiation spectrum. Figure 3 shows the net photoinduced spectrum at 10 K. Clearly, the photoinduced spectrum consists mainly of the A and B' bands. At any temperature there are no clear features other than the A and B' bands: The feature corresponding to B in the ClO_4 salt is missing in the BF_4 salt. In the case of the ClO_4 salt, the B band is an order of magnitude weaker than the B' band.[21] Therefore, the B band might be essentially weak in these substances.

Since the photoinduced bands are asymmetric the log-normal function is employed to decompose the observed spectrum into two bands. As shown in Fig. 3, the asymmetry of an absorption band is measured by the ratio $\rho=d/c$, where c and d are the spectral distances of the half-maximum positions from the peak position ν_0. The full width at half maximum (FWHM) is given by $W=c+d$. Let the maximum absorbance be A_0. Then absorbance of this band is given as a function of frequency ν by[24]

$$A(\nu)=A_0\exp\left[-\frac{\ln 2}{(\ln\rho)^2}\left\{\ln\left[\frac{\nu-\nu_0}{W}\frac{\rho^2-1}{\rho}+1\right]\right\}^2\right], \tag{1}$$

where

$$\nu\gtrless\nu_0-\frac{W\rho}{\rho^2-1} \quad \text{for } \rho\gtrless 1 .$$

Otherwise $A(\nu)=0$. As ρ approaches 1.0, $A(\nu)$ approaches a Gaussian with its FWHM of W. To obtain the values of A_0, ν_0, W, and ρ of the A and B' bands at all temperatures examined, we perform the least-squares fit to the experimental spectra by the iteration method. In Fig. 3 is shown an example of the results. The calculated curve reproduces the experimental spectrum very well.

The integrated intensity of a log-normal absorption band is given by[25]

$$\mathcal{A}\equiv\int_0^\infty A(\nu)d\nu=\left[\frac{\pi}{\ln 2}\right]^{1/2}A_0\xi\ln\rho\theta^{0.5} , \tag{2}$$

with

$$\xi=\frac{W\rho}{\rho^2-1} ,$$

$$\theta=\exp\left\{\frac{(\ln\rho)^2}{2\ln 2}\right\} .$$

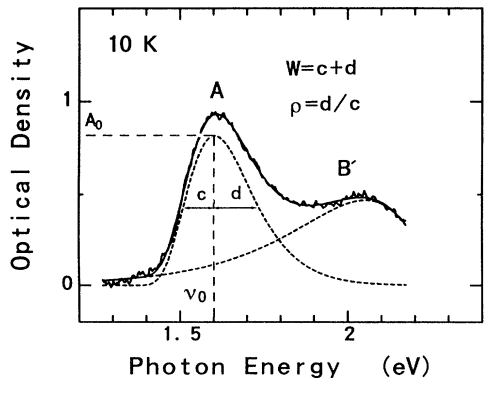

FIG. 3. The photoinduced absorption spectrum at 10 K obtained by subtracting the preirradiation spectrum from the postirradiation spectrum. The smooth solid line is the result of the least-squares curve fit with two log-normal functions shown by dotted lines.

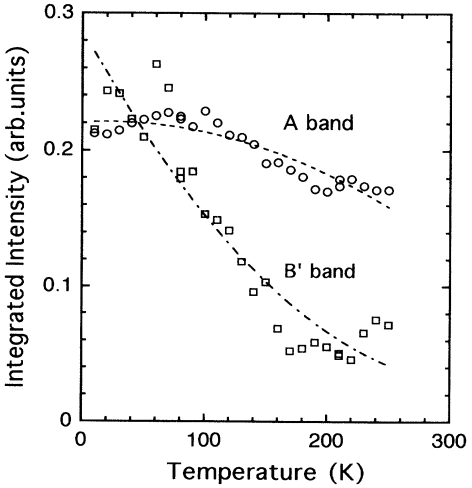

FIG. 4. Temperature dependence of the integrated intensities of the A (○) and B' (□) bands. Dashed lines are drawn as guides.

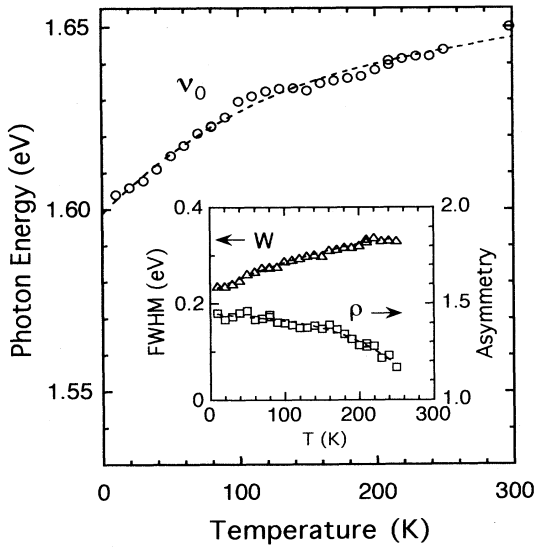

FIG. 5. Temperature dependence of the peak position ν_0 (○), FWHM W (△), and asymmetry parameter ρ (□) of the A band. Dashed lines are drawn as guides.

Figure 4 shows a plot of the integrated intensity of the A and B' bands as a function of temperature. Both bands are reduced with increasing temperature. Experiment needs about 24 h to take all the data presented here. Within this time scale the change of the absorption intensity is reversible upon temperature cycling, in accordance with the very long decay time below 250 K. The result of Fig. 4, therefore, means that the oscillator strength of absorption due to an intragap state depends on temperature. In addition, the temperature dependence differs between the two bands, reflecting that the two bands are associated with different intragap states.

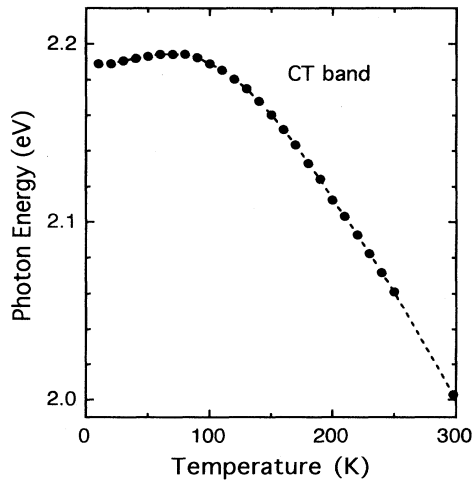

FIG. 6. Temperature dependence of the energy, at which the optical density equals 1.0, of the subgap tail of the CT band. Solid circles are experimental points, and the dashed line is drawn as a guide.

As evident from Fig. 2, the line shape and position of the photoinduced absorption bands vary with temperature. Figure 5 shows the variation of the peak position ν_0, FWHM W, and the asymmetry parameter ρ of the A band with temperature. The peak position turns out to shift continuously from 1.64 to 1.60 eV on cooling the crystal from 250 to 10 K. At the same time, the A band is narrowed to become more asymmetrical in the line shape. The values of the parameters of the B' band scatter largely, particularly at temperatures above 100 K, because of its weak intensity compared to the A band. For the B' band, therefore, the temperature dependencies of the parameters except the integrated intensity are yet to be studied.

Figure 6 shows the photon energy at which the optical density of the CT band of the preirradiation sample is 1.0 as a function of temperature. In contrast to the redshift of the A band with decreasing temperature, the charge-transfer energy gap undergoes a large blueshift, demonstrating the renormalization effect due to a one-dimensional electron-phonon coupling.[26]

In addition, we note from Figs. 5 and 6 that the shifts of the A and CT bands are rather smooth. In the ClO_4 salt the orthorhombic phase, in which the chains are strictly linear, is stable only above 290 K; upon the phase transition at this temperature to the monoclinic phase, in which chains are buckled, the A and CT bands shift discontinuously toward higher energies by 0.02 and 0.04 eV, respectively.[11] Evidently, there are no indications of such anomalies in the data of Figs. 5 and 6 throughout the whole temperature range between 10 and 300 K. Presumably, under 1 atm the orthorhombic phase is unique in the BF_4 salt below room temperature.

IV. DISCUSSION

In this section we shall look closely at the mean energy ν_m, second moment μ_2, and third moment μ_3 of the A band in order to investigate dynamic properties of the midgap state. The log-normal function given by Eq. (1) permits one to calculate ν_m, μ_2, and μ_3. Using the integration formulas derived by Yuan,[25] we obtain

$$\nu_m \equiv \left[\frac{1}{\mathcal{A}}\right]\int_0^\infty \nu A(\nu)d\nu = \nu_0 + \xi(\theta^{1.5}-1)\ , \tag{3}$$

$$\mu_2 \equiv \left[\frac{1}{\mathcal{A}}\right]\int_0^\infty (\nu-\nu_m)^2 A(\nu)d\nu = \xi^2\theta^3(\theta-1)\ , \tag{4}$$

$$\mu_3 \equiv \left[\frac{1}{\mathcal{A}}\right]\int_0^\infty (\nu-\nu_m)^3 A(\nu)d\nu = \xi^3\theta^{4.5}(\theta-1)^2(\theta+2)\ . \tag{5}$$

Figure 7 shows the variations of ν_m, μ_2, and μ_3 of the A band with temperature. All three parameters vary in a similar way to each other, showing a maximum around 120–200 K.

It has been clarified in Sec. III that the energy gap depends on temperature. The temperature dependence of

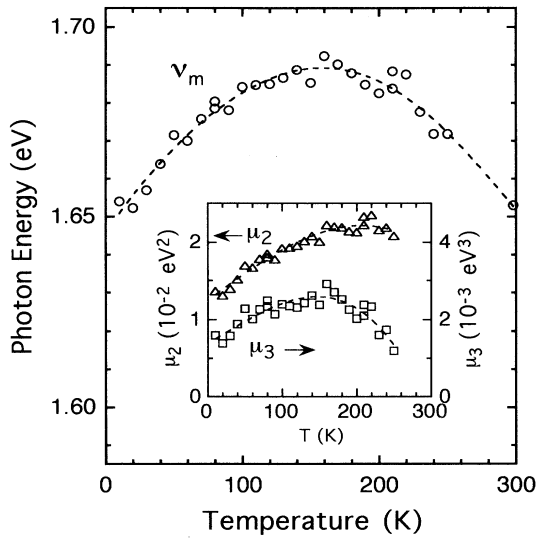

FIG. 7. Temperature dependence of the mean energy ν_m (○), second moment μ_2 (△), and third moment μ_3 (□) of the A band. Dashed lines are drawn as guides.

the energy gap must affect the values of ν_m at high temperatures. A reasonable estimate of this contribution is given by half the temperature-induced shift $\Delta E_{\rm CT}$ of the CT band, since as mentioned in Secs. I and III the A band can be regarded as a midgap band well. Figure 8 shows a plot of the corrected value $\nu_m^c = \nu_m - \frac{1}{2}\Delta E_{\rm CT}$. Of course, since the CT band should broaden thermally, $\Delta E_{\rm CT}$ should be greater than the shift of the energy gap itself, and thus the values of ν_m^c at high temperatures might be appreciably overestimated. It may be safe, however, to say that if the energy gap remains unchanged ν_m

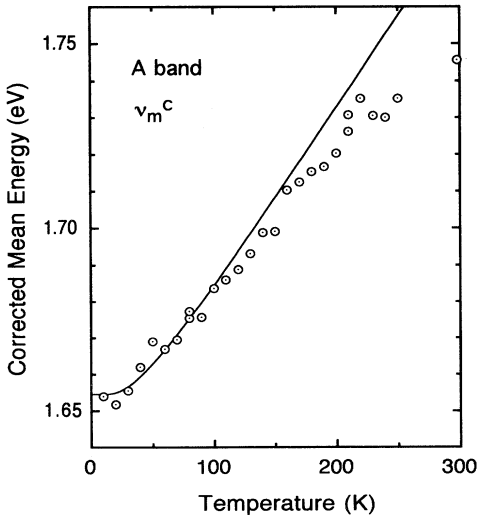

FIG. 8. Temperature dependence of ν_m^c. The marks ○ are the experimental points, and the solid line is the theoretical curve calculated from Eq. (8).

continues to increase with increasing temperature beyond 100 K. In addition, even at 10 K both the damping factor $\sqrt{\mu_2}$ and the asymmetry factor $\sqrt[3]{\mu_3}$ exceed 0.1 eV, which is much greater than the thermal energy. Moreover, they increase further as temperature increases.

In general, quantum fluctuations in a specific configuration-coordinate space cause the absorption band of a localized center to have a large damping and asymmetry. To a first approximation one may express the potentials of the ground and excited states, between which the optical transition takes place, around an optimum position as

$$U_e = \nu_e + \tfrac{1}{2}\omega_e^2 (r-\Delta)^2 , \tag{6}$$

$$U_g = \tfrac{1}{2}\omega_g^2 r^2 , \tag{7}$$

where the mass and Planck's constant are set unity. The quantities ω_g and ω_e are the eigenfrequencies of fluctuation in the ground and excited states, respectively, ν_e is the difference in energy between the minima of the potentials, and Δ is the relative displacement of the minima along the configuration coordinate r. According to Siano and Metzler,[27] assuming an infinite series of the harmonic-oscillator levels,

$$\nu_m = \nu_e + \tfrac{1}{2}\omega_e^2\Delta^2 + \frac{(\omega_e^2-\omega_g^2)}{4\omega_g}\coth\left[\frac{\omega_g}{2kT}\right] , \tag{8}$$

$$\mu_2 = \frac{\omega_e^4\Delta^2}{2\omega_g}\coth\left[\frac{\omega_g}{2kT}\right] + \frac{(\omega_e^2-\omega_g^2)^2}{8\omega_g^2}\coth^2\left[\frac{\omega_g}{2kT}\right] , \tag{9}$$

$$\mu_3 = \frac{3\omega_e^4\Delta^2(\omega_e^2-\omega_g^2)}{4\omega_g^2}\coth^2\left[\frac{\omega_g}{2kT}\right] + \frac{(\omega_e^2-\omega_g^2)^3}{8\omega_g^3}\coth^3\left[\frac{\omega_g}{2kT}\right] , \tag{10}$$

where k is the Boltzmann constant and T is the temperature. Equations (8)–(10) predict that the quantities ν_m, μ_2, and μ_3 are correlated intimately to one another, and that they vary monotonically with temperature. It is apparent from the experimental results that in the present case $\omega_e > \omega_g$.

Let us examine the experimental results quantitatively on the basis of this theory. The data of μ_2 and μ_3 suggest that the simple harmonic-oscillator picture is valid only below about 100 K. Thus we restrict the discussion to this low-temperature regime. Since the energy gap is almost constant below 100 K, Eq. (8) may apply to the change in ν_m observed. In fact a good fit of Eq. (8) to those data of ν_m is given by $\omega_g = (9.5\pm2.0)\times10^{-3}$ eV, $\omega_e/\omega_g = 3.5\pm0.4$, and $\nu_c = 1.625\pm0.005$ eV, where

$$\nu_c = \nu_e + \frac{\omega_e^2\Delta^2}{2} . \tag{11}$$

This value of ω_g suggests that the midgap states fall mostly into the zero-point level below 100 K. In Fig. 8

the theoretical curve calculated with $\omega_g = 8.4 \times 10^{-3}$ eV, $\omega_e/\omega_g = 3.6$, and $\nu_c = 1.63$ eV is shown along with the data of ν_m^c. The reason for the discrepancy, which is seen between the theoretical and experimental values of ν_m^c at high temperatures, will be discussed below.

To test the correlation of μ_2 and μ_3 with ν_m, it is convenient to rewrite Eqs. (9) and (10) as

$$\mu_2 = \mu_{2d} + a(\nu_m - \nu_c) + 2(\nu_m - \nu_c)^2 , \quad (12)$$

$$\mu_3 = \mu_{3d} + 6a(\nu_m - \nu_c)^2 + 8(\nu_m - \nu_c)^3 , \quad (13)$$

with

$$a = \left[\frac{4\omega_e^2}{\omega_e^2 - \omega_g^2} \right] \left[\frac{\omega_e^2 \Delta^2}{2} \right] , \quad (14)$$

where the constants μ_{2d} and μ_{3d} are incorporated into this analysis to take the static disorder effects into account. Figure 9 shows a plot of the data of μ_2 and μ_3 below 100 K as a function of ν_m. Reasonable agreement of Eqs. (12) and (13) with the data can be obtained with $\mu_{2d} = (1.0 \pm 0.2) \times 10^{-2}$ eV^2, $\mu_{3d} = (0.7 \pm 0.3) \times 10^{-3}$ eV^3, and $a = 0.07 \pm 0.01$ eV. Putting the value of a into Eq. (14), we obtain $\omega_e^2 \Delta^2/2 = 0.016 \pm 0.002$ eV. Hence Eq. (11) gives $\nu_e = 1.60$ eV. In Fig. 9 the theoretical curves of μ_2 and μ_3 calculated from Eqs. (12) and (13), respectively, with $\mu_{2d} = 1.1 \times 10^{-2}$ eV^2, $\mu_{3d} = 1.0 \times 10^{-3}$ eV^3, $a = 0.06$ eV, and $\nu_c = 1.63$ eV are compared to the experimental data.

It appears from this analysis that the temperature dependencies of various spectroscopic aspects of the A band in a range of 10–100 K are explained consistently in terms of quantum fluctuations: The eigenfrequencies of the ground and excited states are found to be of the order of 10 and 30 meV, respectively. Based on the site-diagonal electron-lattice coupling scheme,[28,29] which assumes that the electron-lattice coupling is dominated by the in-chain displacement of halogen ions relative to Pt ions, the in-chain local vibrations of Cl^- ions might be

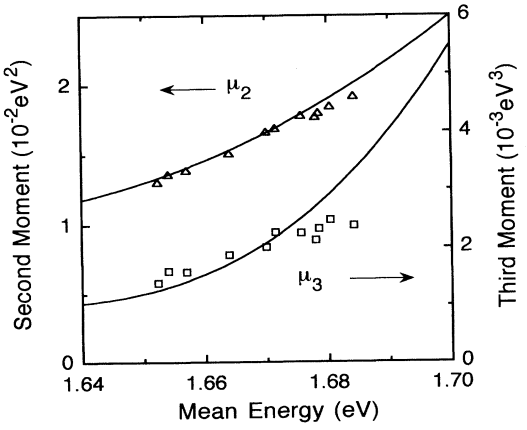

FIG. 9. Plot of second moment μ_2 (△) and third moment μ_3 (□) of the A band as a function of the mean energy ν_m. The solid lines are theoretical curves of μ_2 vs ν_m and μ_3 vs μ_m calculated from Eqs. (13) and (14), respectively.

ingredients for the quantum fluctuation. The frequencies, however, of the Raman-active local modes are 32–36 meV,[30,31] being greater than the value of ω_g by a factor of 3–4.

A more possible origin of the quantum fluctuation is the vibration of the entire local state. The frequency of the in-chain vibration of the Pt-Cl-Pt unit of a spin soliton, for instance, is estimated to be $\sim \omega_0 \sqrt{M_{Cl}/(2M_{Pt} + M_{Cl})} = 11$ meV, in good agreement with ω_g, where ω_0 is the frequency, 38.6 meV,[15] of the breathing mode of Cl^- ions, and M_{Cl} and M_{Pt} are the atomic masses of Cl and Pt, respectively. This mode would couple strongly with the localized electrons because the restoring force comes from the Cl^- ions holding the Pt-Cl-Pt unit from both sides. Consequently, the spin distribution would fluctuate, as shown by EPR in the ClO_4 salt,[6] so as to be synchronized with the vibration.

Another possible origin is the vibration of the soliton itself around the equilibrium position. The spin soliton in the present substance has an effective mass of about $300m_0$,[21,32] where m_0 is the free-electron mass: Such a large effective mass is essential to a soliton of an MX chain complex because fluctuations of halogen ions are always linked with the motion of the soliton. The solitons are subjected to a shallow periodic potential with a periodicity of twice the nearest Pt-Pt distance.[33,34] To estimate the vibration frequency let the potential be a sinusoidal function of the position, and the depth be 20–40 meV. Then the frequency of the zero-point motion turns out to be 9–13 meV, assuring that at low temperatures the solitons can be bound by a well of the potential; the eigenfrequency 18–26 meV is comparable to the value of ω_g.

Now we turn our attention to the data above 100 K. Contrary to the prediction of the configuration-coordinate model, the second and third moments μ_2 and μ_3 of the A band level off around 120–200 K and then decrease with increasing temperature. An interpretation of this anomalous phenomenon has been put forward with the thermally activated random walk of solitons taken into account.[21,22] As postulated in the arguments presented in the preceding paragraph, the periodic potential for a soliton, particularly for the spin soliton, could not be deep enough to confine a soliton firmly within a certain well. Consequently, solitons may move along the chain bonds at elevated temperatures. Since the potential of the excited state must also be periodic with a depth comparable to that of the ground state, the local fluctuation effect is eventually smeared out at high temperatures, and thus the second and third moments would approach their ordinary values. It may also be true for ν_m^c. In fact, as seen in Fig. 8, the higher the temperature the larger the downward deviation of ν_m^c from the theoretical curve. The thermal broadening effect of the CT band is ignored in deriving ν_m^c. Therefore the actual deviation might be appreciably larger than the deviation seen in Fig. 8.

A soliton of an MX chain complex changes its own valence structure while moving along the chain.[33] The structure of a spin soliton, for instance, is changed from

$Pt^{2.5}$-Cl^--$Pt^{2.5}$ to Cl^--Pt^3-Cl^- and $Pt^{3.5}$-Cl^--$Pt^{3.5}$ successively on going from an optimum site to the midpoint toward the next optimum site. Presumably, such a change contributes additionally to the anomalous behaviors of ν_m, μ_2, and μ_3 at elevated temperatures. The pronounced temperature dependence of the oscillator strength may also be related to this property.

V. SUMMARY

The effect of laser irradiation on the optical absorption has been studied in single crystals of an *MX* chain complex $[Pt(en)_2][Pt(en)_2Cl_2](BF_4)_4$, where (en) is ethylenediamine. The midgap band, which appears in the pristine crystal around 1.6 eV, is found to be strengthened efficiently by the irradiation with the 488-nm line of an Ar laser. In addition, a broad band is induced around 2.0 eV. The two bands correspond well in energy and line shape to the *A* and *B'* bands, respectively, in the ClO_4 salt. It may be concluded, therefore, that the two bands are associated with different intragap states. However, the absorption corresponding to the *B* band in the ClO_4 salt is absent in the present substance.

The *A* and *B'* bands, induced by laser irradiation at 250 K, persist as long as the temperature is kept below 250 K. The spectra of the two bands show significant changes in the position, line shape, and intensity if the temperature is lowered from 250 to 10 K. The intensity is reversible upon temperature cycling for both bands: Because the two bands arise from different states the temperature dependencies of their intensity are significantly different from one another. The mean energy and second and third moments have been evaluated, with attention paid to the *A* band. A quantitative analysis of the results on the basis of the configuration-coordinate model manifests that the photoinduced midgap states undergo a certain quantum fluctuation at low temperatures with its eigenfrequency of the order of 10 meV, and that they walk randomly at elevated temperatures. Possible origins of the quantum fluctuation have been discussed in the light of a strong site-diagonal coupling between the electrons of the localized states and the in-chain displacement of Cl^- ions.

Spectroscopically, the orthorhombic phase appears to be stable in this substance throughout the temperature range between 10 and 300 K. Nevertheless the properties of the midgap states found by the present study are essentially identical with those of the monoclinic phase in the ClO_4 salt, suggesting that it is not crucial to the properties of the midgap states whether the *linear* chains of the Pt-Cl bonds are straight or buckled.

ACKNOWLEDGMENT

N.K. and M.N. acknowledge Dr. N. Matsushita of Tokyo University for valuable discussions.

*Present address: Sony Co., Kitashinagawa 6-7-35, Shinagawa-ku, Tokyo 141, Japan.

[1]N. Matsushita, H. Kitagawa, and T. Mitani, Synth. Met. **71**, 1933 (1995).
[2]K. Toriumi, M. Yamashita, S. Kurita, I. Murase, and T. Ito, Acta Crystallogr. Sec. B **47**, 497 (1993).
[3]H. Okamoto, T. Mitani, K. Toriumi, and M. Yamashita, Mater. Sci. Eng. B **13**, L9 (1992).
[4]M. Alouani, J. W. Wilkins, R. C. Albers, and J. M. Wills, Phys. Rev. Lett. **71**, 1415 (1993).
[5]N. Kuroda, M. Sakai, M. Suezawa, Y. Nishina, and K. Sumino, J. Phys. Soc. Jpn. **59**, 3049 (1990).
[6]M. Sakai, N. Kuroda, M. Suezawa, Y. Nishina, K. Sumino, and M. Yamashita, J. Phys. Soc. Jpn. **61**, 1326 (1992).
[7]N. Kuroda, M. Ito, Y. Nishina, A. Kawamori, Y. Kodera, and T. Matsukawa, Phys. Rev. B **48**, 4245 (1993).
[8]R. Ikeda, A. Ghosh, L. S. Prabhumirashi, D. Nakamura, and M. Yamashita, Mol. Cryst. Liq. Cryst. **216**, 181 (1992).
[9]N. Matsushita, N. Kojima, T. Ban, and I. Tsujikawa, J. Phys. Soc. Jpn. **56**, 3808 (1987).
[10]N. Mastushita, N. Kojima, N. Watanabe, and T. Ban, Solid State Commun. **71**, 253 (1989).
[11]M. Sakai, N. Kuroda, and Y. Nishina, Phys. Rev. B **40**, 3066 (1989).
[12]F. H. Long, S. P. Love, and B. I. Swanson, Phys. Rev. Lett. **71**, 762 (1993).
[13]S. Kurita, M. Haruki, and K. Miyagawa, J. Phys. Soc. Jpn. **57**, 1789 (1988).
[14]N. Kuroda, M. Ito, Y. Nishina, and M. Yamashita, J. Phys. Soc. Jpn. **62**, 2237 (1993).
[15]N. Kuroda, M. Nishida, N. Matsushita, and M. Yamashita, Synth. Met. **71**, 1921 (1995).
[16]N. Kuroda, M. Sakai, Y. Nishina, M. Tanaka, and S. Kurita, Phys. Rev. Lett. **58**, 2122 (1987).
[17]H. Okamoto, T. Mitani, K. Toriumi, and M. Yamashita, Phys. Rev. Lett. **69**, 2248 (1992).
[18]J. Gammel, A. Saxena, I. Batistic, and A. R. Bishop, Phys. Rev. B **45**, 6408 (1992); S. M. Milbrodt, J. Gammel, A. R. Bishop, and E. Y. Loh, *ibid.* **45**, 6435 (1992).
[19]I. Batistic, X. Z. Huang, A. R. Bishop, and A. Saxena, Phys. Rev. B **48**, 6065 (1993).
[20]K. Iwano and K. Nasu, J. Phys. Soc. Jpn. **61**, 1380 (1992).
[21]N. Kuroda, M. Ito, and M. Yamashita, Phys. Rev. B **50**, 8063 (1994).
[22]N. Kuroda, M. Ito, Y. Nishina, and M. Yamashita, Mol. Cryst. Liq. Cryst. **256**, 885 (1994).
[23]N. Matsumoto, M. Yamashita, and S. Kida, Bull. Chem. Soc. Jpn. **51**, 2334 (1978).
[24]D. E. Metzler, C. M. Harris, R. J. Johnson, and J. A. Thomson, Biochemistry **12**, 5377 (1973).
[25]P. Yuan, Ann. Math. Stat. **4**, 30 (1933).
[26]N. Kuroda, M. Nishida, and M. Yamashita (unpublished).
[27]D. B. Siano and D. E. Metzler, J. Chem. Phys. **51**, 1856 (1969).
[28]K. Nasu, J. Phys. Soc. Jpn. **52**, 3865 (1983).
[29]D. Baeriswyl and A. R. Bishop, Phys. Scr. **T19**, 239 (1987).
[30]S. C. Huckett, R. J. Donohoe, L. A. Worl, A. D. Bulou, C. J. Burns, J. R. Laila, D. Carrol, and B. I. Swanson, Chem. Mater. **3**, 123 (1992).
[31]S. P. Love, L. A. Worl, R. J. Donohoe, S. C. Huckett, S. R. Johnson, and B. I. Swanson, Synth. Met. **55-57**, 3456 (1993).
[32]Y. Onodera, J. Phys. Soc. Jpn. **56**, 250 (1987).
[33]N. Kuroda, M. Kataoka, and Y. Nishina, Phys. Rev. B **44**, 13260 (1991).
[34]M. Suzuki and K. Nasu, Phys. Rev. B **45**, 1605 (1992).